International Journal of Applied Earth Observation and Geoinformation 128 (2024) 103699

Contents lists available at ScienceDirect

International Journal of Applied Earth Observation and Geoinformation

journal homepage: www.elsevier.com/locate/jag

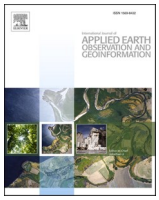

Characterising maize and intercropped maize spectral signatures for cropping pattern classification

Mbali Mahlayeye [a,*], Roshanak Darvishzadeh [a], Andrew Nelson [a]

[a] Faculty of Geo-information Science and Earth Observation (ITC), University of Twente, Enschede 7500AE, The Netherlands

ARTICLE INFO

Keywords:
Cropping patterns
Intercropping
Sentinel-2
Random Forest classification

ABSTRACT

Intercropping – the planting of more than one crop in the same plot of land – is a prevalent agricultural management practice which can be used for risk reduction. Despite its widespread use, intercropping is not commonly reported in agricultural statistics, resulting to very limited spatially disaggregated information about its prevalence. Remote sensing-based approaches to detect and estimate the area of cropping patterns like intercropping require good understanding of the spectral response of (intercropped) crops at different crop growth phases. This study integrates field surveys, farmer interviews and temporal Sentinel-2 data from four crop growth phases and the post-harvest period of maize and intercropped maize (imaize). The goal is to identify the optimal crop growth phases, spectral regions and vegetation indices (VIs) that can accurately discriminate the two cropping patterns. We computed *p*-values for the spectral bands using Mann-Whitney *U* test and identified critical crop growth phases. Classification of maize and imaize cropping patterns was performed using random forest classifier. Our spectral analysis revealed effective discrimination between maize and imaize cropping patterns during the vegetative (in all spectral bands) and flowering-yield phases (in Blue, Green, Red, RE704, RE783, NIR833, NIR865). The most suitable VIs contained red-edge and near-infrared spectal bands. Utilizing spectral data and VIs from vegetative and flowering-yield phases, we achieved optimal discrimination during the vegetative phase (user's accuracy of 100 % and producer's accuracy of 100 %). However, accuracy decreased during the flowering yield phase (overall accuracy of 87 % for all spectral bands). The highest classification results using all spectral bands at the flowering yield phase resulted in 80 % producer's accuracy for maize and 100 % for imaize. This study illustrates the utility of temporal Sentinel-2 spectral data for identifying the critical crop growth phase, spectral regions and VIs for cropping patterns classification, particularly for intercropping.

1. Introduction

Intercropping, the planting of more than one crop in the same plot of land, is predominantly practised to maximise land use and crop diversity, and to mitigate the risk of yield loss (Giller et al., 2021b; Himmelstein et al., 2017). Intercropping is associated with weed reduction, the control of pests and diseases (Bybee-Finley and Ryan, 2018; Zaefarian and Rezvani, 2016), the preservation of soil nutrients and reduction of rainwater runoff (Sun et al., 2019; Yang et al., 2020). It can also promote biodiversity (Liu and Chen, 2019), sustain food production, and diversify income (Zuo et al., 2013). According to Himmelstein et al. (2017), on average intercropping can increase crop yields by 23 %.

There are different types of intercropping, and the practice of intercropping is dynamic, evolving with seasonal changes and the availability of external resources (Kehs et al., 2021). Intercropping types can be described based on the arrangement of the crops within a field; mixed, strip and row cropping (Bégué et al., 2018; Mahlayeye et al., 2022). The spatial and temporal dynamics in intercropping practice and the different types of intercropping show that it is challenging to generate reliable and timely information on when, where, and how intercropping practice is practiced.

Intercropping is the backbone of African agriculture, though such practice is not commonly reported in agricultural statistics and spatially disaggregated information about the location of intercropping is not available (Giller et al., 2021a). In Africa, between 41 % and 86 % of maize, rice, sorghum, and millet are estimated to be produced from intercropped fields (Garrett et al., 2020), but this depends on management practices and agro-ecological factors. More spatially detailed estimation of intercropped area requires robust mapping and monitoring approaches.

* Corresponding author.
E-mail addresses: m.mahlayeye@utwente.nl (M. Mahlayeye), r.darvish@utwente.nl (R. Darvishzadeh), a.nelson@utwente.nl (A. Nelson).

https://doi.org/10.1016/j.jag.2024.103699
Received 21 June 2023; Received in revised form 26 January 2024; Accepted 30 January 2024
Available online 13 February 2024

The spatial, spectral, and temporal resolution of imagery such as Sentinel-1, Sentinel-2, RapidEye, and WorldView-2 (Bégué et al., 2020) may provide suitable information for identifying intercropping practices yet studies on intercropping are rare. Most studies have focused on mapping the crop type and cropping patterns of single cropped fields, occasionally accompanied by intercropped fields, and have used a single satellite image during one crop growing season or spectral information from different growth phases when using multiple dates (Aduvukha et al., 2021; Hegarty-Craver et al., 2020; Ibrahim et al., 2021; Richard et al., 2017). A common observation of these studies is that intercropped fields tend to have a similar spectral response to single crop fields, resulting in misclassification. Consequently, intercropped fields have often been misclassified in previous studies (Gumma et al., 2020; Hegarty-Craver et al., 2020). One of the studies that explored multi-temporal data for intercropping mapping was by Ibrahim et al. (2021). That study used Sentinel-2 to map maize in single-cropped and intercropped fields using phenological analysis and crop calendars to find useful temporal windows/periods for discriminating different cropping patterns. However, these windows were not clearly linked to crop type and crop growth phases, further, each separation window identified seem to cover multiple crop growth phases.

Several methods have been used for cropping pattern classification, including the fusion of multi-sensor data (Chen et al., 2014; Ding et al., 2020; Ferrant et al., 2019), object-based classification technigues (Cui et al., 2020; Song et al., 2017), and a combination of object and pixel-based classification using various algorithms (Belgiu and Csillik, 2018; Castillejo-González et al., 2009). The majority of these studies have explored different classification methods, with machine learning methods being the most preferred approach. Notably, mainly Random Forest (RF) and Support Vector Machine (SVM) have demonstrated superior perfomance in achieving high classification accuracies (Kuchler et al., 2020; Liu et al., 2013; Liu and Chen, 2019). Despite their effectiveness, the results of machine learning methods, including RF and SVM, can be inconsistent (Feyisa et al., 2020). Several factors contribute to the variability, including hyperparameter tuning (Saini and Ghosh, 2018), sample quality and quantity (Jin et al., 2019), selection of training samples (Belgiu and Drăgu, 2016), imbalanced classes (Belgiu et al., 2021) and feature selection (Peña-Barragán et al., 2011). Achieving optimal model performance often involves a trade-off among these factors, necessitating experimentation to fine-tune the models (Belgiu and Drăgu, 2016). The accuracy of mapping is also influenced by the common practice of using a generalized approach for mapping different crop types and cropping patterns. In regions characterized by substantial diversity in cropping practices and varying field-level cropping patterns, misclassification issues may arise. This approach is suitable when there are enough field boundaries for different categories at the field level. Therefore, starting with a field-based approach can enhance our understading of the factors contributing to these misclassifications and improve classification accuracy.

Comprehensive understanding and consideration of various factors are essential for obtaining precise spatial information about cropping patterns. To enhance the accuracy of mapping maize cropping patterns, it is crucial to have knowledge of the multiple factors that contribute to their complexity. Key factors, including cropping practices such as weed control (Ibrahim et al., 2021), synchronized crop calendar data, and the management of pests and diseases (Mthembu et al., 2019), play a crucial role in successfully distinguishing these cropping patterns. These factors provide valuable guidelines for selecting suitable remote sensing data and methods, which are instrumental in achieving precise classification and generating reliable spatial information.

According to Mahlayeye et al. (2022), no studies have explored and separately analysed the spectral response of cropping patterns that include intercropping at different crop growth phases. The use of multi-temporal Sentinel-2 data throughout the entire crop growing season to identify the most suitable crop growth periods phases for improved classification of single-cropped and intercropped cropping patterns has not been explored.

The objective of this study is to analyze the variations in Sentinel-2 spectral signatures of maize and intercropped maize (imaize) at a field-level during the crop growing season. This analysis includes spectral discrimination and classification of maize and imaize cropping patterns.

2. Materials and methods

2.1. Study area

The Busia County was selected as the study area and is located in the western region of Kenya (Fig. 1). Its central coordinates are 0°27′38.77″N and 34°06′41.26″E and it borders Uganda to the West and Lake Victoria to the Southeast. The area of interest spans about 950 km square and it is within three agroecological zones (AEZs); Lower Midland Sugarcane Zone (LM1), Marginal Sugarcane Zone (LM2), and Lower Midland Cotton Zone (LM3) (Jaeztold, 1983). Busia has a tropical rainforest climate, the temperature ranges from 17 − 28 °C with an average annual precipitation of 302 mm and 307 (84 %) rainy days per year. There are two rainy seasons, resulting in a bimodal rainfall pattern. The long rains start between March-April and short rains around October-November. Farming is predominantly rainfed with farmers planting in February-March (first crop growing season) and again in August-September (second crop growing season) (Fig. 3).

Maize is the dominant crop in the region, cultivated either as monocrop, generally for commercial purposes, or as an intercrop typically for subsistence consumption, alongside beans, soybeans, cowpea, and cassava. Other crops found in the region include millet, groundnut, and sorghum. The prevalent cropping patterns are maize and imaize. The dominant intercropping type is mixed and row intercropping (Fig. 2).

2.2. Data

Farmer interviews, field boundaries, crop type, crop calendar information, and Sentinel-2 images were utilized to characterise imaize and maize cropping patterns. We implemented a stratified random sampling method for our study, taking into account crop calendars, crop types, and cropping patterns. Additionally, we utilized secondary field data provided by Plant Village, an initiative affiliated with Penn State University, which strives to uplift small-scale farmers from poverty by making technology, data and information about crop cultivation more accessible for farmers, government and researchers (Plant Village, 2023). Notably, a significant proportion of farmers in the study area primarily cultivated maize, either as a sole crop or in intercropping with legumes. To ensure an adequate sample size, we focussed our sampling efforts on the most prevalent crop types and cropping patterns.

(i) Farmer interviews

In July 2022 we interviewed 240 farmers from the northern parts which includes Teso North, Teso South and Nambale sub-counties. Farmer interviews were based on the first and second crop growing season's management practices from year 2019 till 2022. Questions included field sizes, the variety of crops cultivated in both long rain and short rain seasons, the specific timelines of planting and harvesting for each crop, the categorization of intercropping types (mix, strip, row), planting techniques, encountered challenges (such as drought and crop health issues), factors that influence the choice of cropping patterns, and crop management practices (including crop varieties, weed control, pesticide application, fertilizer application, etc.). Prior to the interviews, the farmers provided informed oral consent and had the option to terminate the interview at any given moment.

The majority of the farmers recalled the months for both planting and harvesting, providing either precise dates or approximate time frames (early/late). Notably, farmers adopt various maize varieties bi-

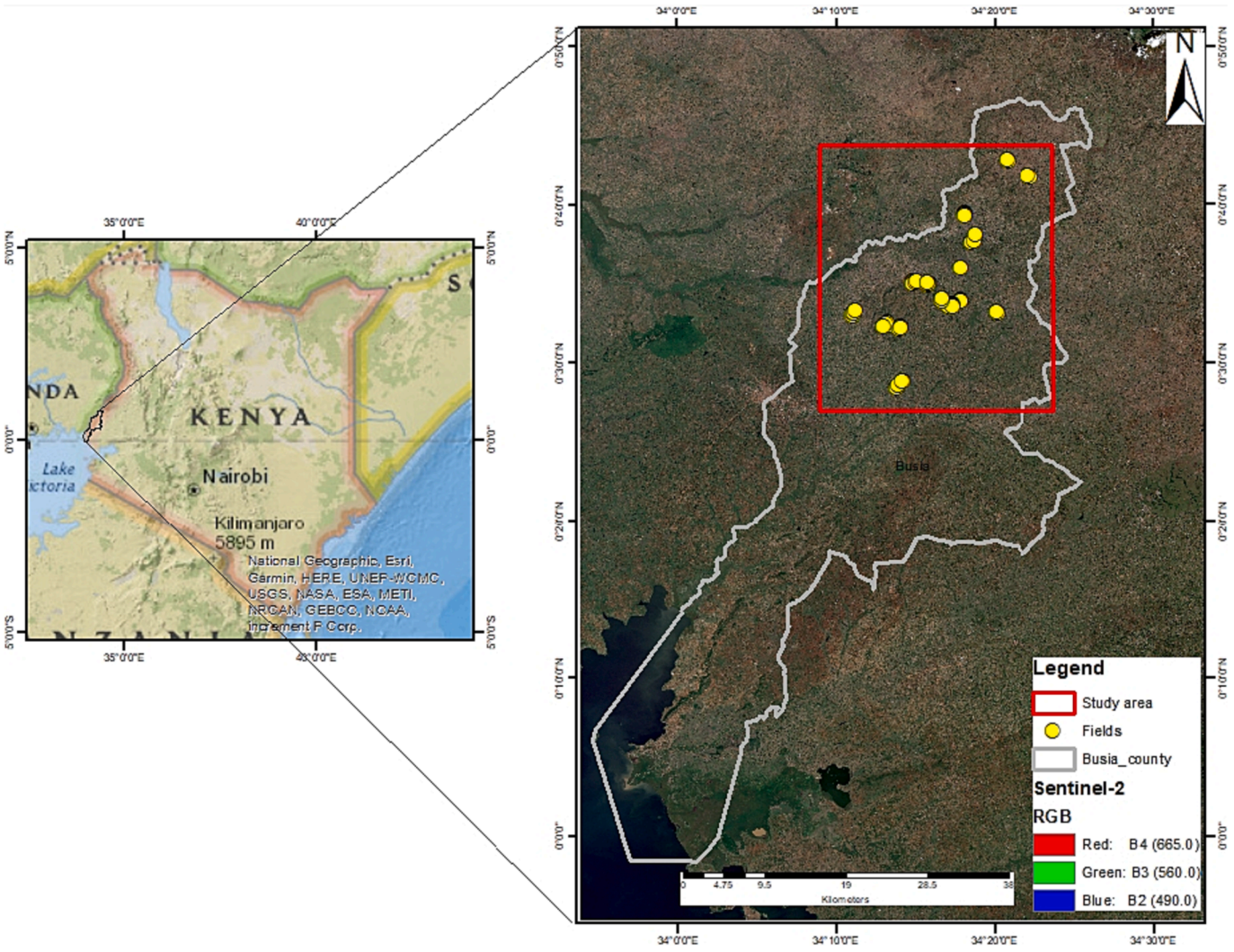

Fig. 1. Study area, Busia in western Kenya.

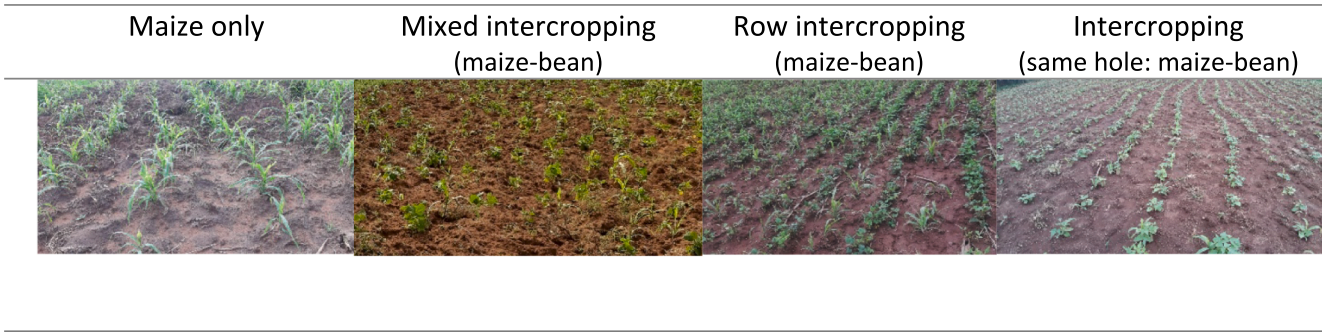

Fig. 2. Emergence-seedling phase of maize cropping patterns.

annually to optimize their yield. These varieties commonly mature after 90–120 days. Manual harvesting is prevalent in this region and the residual maize plants are often left in the field as fodder for cattle.

(ii) Field boundaries

Field boundaries for 2019, delineated by PlantVillage - a project by Penn State University- in partnership with Radiant Foundation, they strive to assist small-scale farmers by using affordable technology and making data and information more accessible. The primary objective is to aid farmers in improving food production and overcoming poverty. These field boundaries were verified during our field visit and were adjusted or eliminited if they no longer accurately depicted the actual situation or if farmers provided different information. A total of 120 fields were visited, and 87 of these were considered for this study: 50 comprised of maize fields and 37 were categorized as imaize fields. The GPS coordinates of these field boundaries were updated from PlantVillage data, with some being newly recorded on-site using Map Marker application (www.mapmarker.app). These coordinates were later verified using high-resolution images from Google Earth. Field observations,

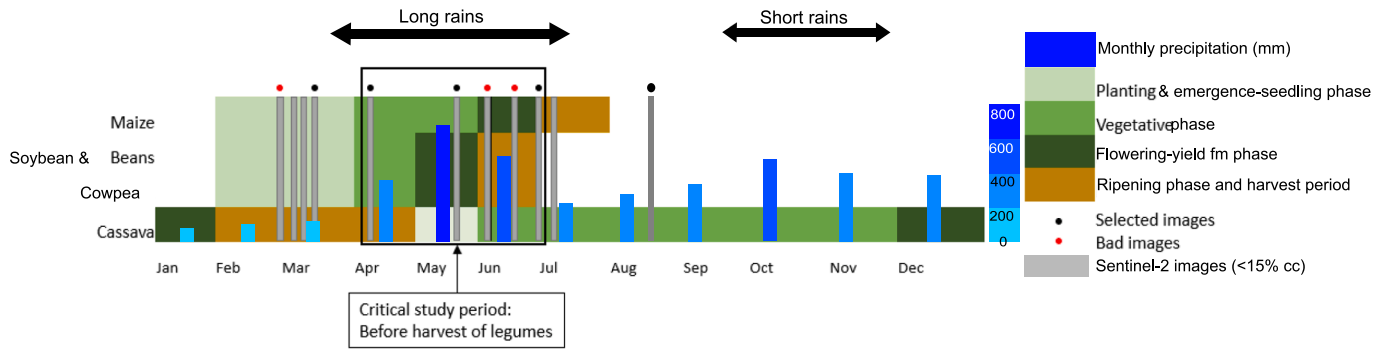

Fig. 3. Crop calendar showing critical period, crop growth phases, available satellite images, 2019 average monthly precipitation of Busia.

photographs and sketches of the fields were used to document the locations of trees and any objects that could potentially influence the reflectance response within these fields.

(iii) Crop type, phases, and crop calendar

The field boundary data provided by Plant Village encompassed crop calendar information with only planting and estimated harvest dates (Plant Village, 2019). These were revised following interviews with farmers. Our focus was on the first long-rain season due to its extended crop growth period and the prevalence of intercropping among most farmers, as indicated by the interviews. Furthermore, during this period, farmers allocate more resources, anticipating higher yields compared to the subsequent short-rain season. Notably, in this region, the impacts of climate change are predominantly experienced during the second season. Table 1 describes the considered maize growth phases and their relation to land-surface phenology derived from remote sensing-based information.

(iv) Sentinel-2 time-series images

The Sentinel-2 Multispectral Imager (MSI) has 13 spectral bands in the visible (VIS), red-edge (RE), near-infrared (NIR) and shortwave infrared (SWIR) domains. Sentinel-2 images were attained from March to August 2019, selecting scenes with less than 15 % cloud cover and a UTM/WGS84 projection. The dates on which images were acquired and utilized were: 23rd March, 12th April, 22nd May, 01st July, and 25th August 2019. No cloud masking was necessary as the study area remained cloud-free during these dates. The images were surface reflectance (SR) (level 2A) corrected from the Copernicus Open Access hub. (Fig. 3).

During pre-processing, B1, B9, and B10 were excluded as they were not relevant to this study (Table 2). We used the SNAP toolbox to resample B5, B6, B7, B8A, B11 and B12 from 20 m to 10 m. Upon stacking the 10 m bands, the ENVI software (ENVI version 5.6.3. Harris Geospatial, USA) was used for processing and analyzing geospatial data. This software facilitated the computation of the average spectral reflectance and standard deviation using the field boundaries. Maize and imaize field spectral signatures were computed according to crop growth phases, from emergence-seedling to ripening and post-harvest period (Fig. 4).

Table 1
Maize growth stages and definitions (adopted from (FAO, 2022)).

Maize growth phase	Definition	Phenology phase
Emergence-seedling (15–25 days)	Development of leaves and appearance of leave collars	Green up
Vegetative (25–40 days)	Elongation of the stem, dominant nodal root system	Early-phase
Flowering-Yield formation (20–40 days)	Development of maize cob and tassel	Mid-late phase
Ripening (10–15 days)	Kernels fully developed, ready for harvest	Late phase

Table 2
Sentinel-2 spectral bands used.

Spectral bands	Central wavelength (nm)	Spatial resolution (m)
Band 2 – Blue	492	10
Band 3 – Green	560	10
Band 4 – Red	665	10
Band 5 – RE	704	20
Band 6 – RE2	740	20
Band 7 – RE3	783	20
Band 8 – NIR	833	10
Band 8A –NIR2	865	20
Band 11 – SWIR1	1614	20
Band 12 – SWIR2	1374	20

2.3. Analysis of spectral signatures of single and intercropping maize fields

We extracted the average reflectance values from Sentinel-2 images for each field, categorizing them into maize and imaize. A comprehensive time-series analysis on Sentinel-2 data was then performed to understand differences between maize and imaize fields. Firstly, we explored the influence of phenological phases on the spectral reflectance differences within maize cropping patterns. Four main growth phases-emergence-seedling, vegetative, flowering-yield formation, and ripening- were carefully selected. We calculated average reflectance, standard deviation, the first derivative of every growth phase, then computed line and boxplots for every spectral region for maize and imaize cropping patterns.

The Mann-Whitney *U* test was used for all crop growth phases and post-harvest period, to identify significant differences in spectral reflectance between maize and imaize cropping patterns, since our data were not normally distributed. The test is non-parametric and can be compared to the *t*-test; however, it relies on no assumptions about the data distribution.

2.4. Temporal analysis using various VIs

We considered the following VIs, which are commonly used for temporal and phenological analysis of vegetation (Table 3) and which predominantly use red-edge and near-infrared bands. The findings from 2.3 were used to further refine this list of VIs and identify the most promising ones.

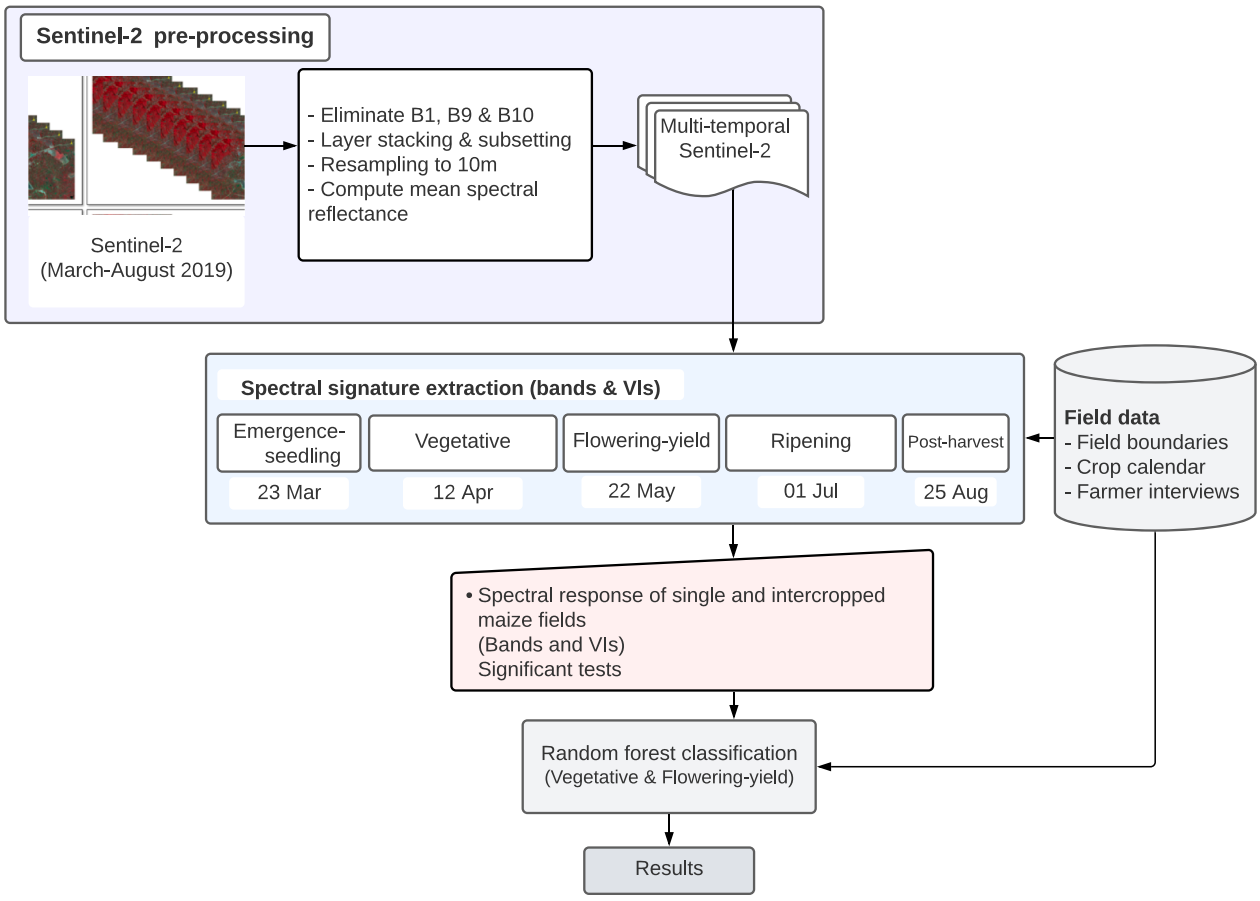

Fig. 4. Methodological flowchart for the discrimination and classification of single and intercropped maize.

Table 3
List of indices used for phenological temporal analysis of the spectral response of maize and imaize.

Index	Formula	Description	Reference
NDVI	(NIR − R)/(NIR + R)	Normalized Difference Vegetation Index	(Rouse et al., 1973)
NDWI	(G − NIR)/(G + NIR)	Normalized Difference Water Index	(McFeeters, 1996)
NDRE2	(NIR − RE2)/(NIR + RE2)	Red Chlorophyll Index	(Gitelson and Merzlyak, 1994; Kross et al., 2015)
NDRE	(NIR − RE)/(NIR + RE)	Normalized Difference Red-edge Index	(Kross et al., 2015)
GNDVI	(NIR − G)/(NIR + G)	Green Normalized Difference Vegetation Index	(Gitelson and Merzlyak, 1998)
SIPI	(NIR − B)/(NIR + R)	Structure Intensive Pigment Vegetation Index	(Peñuelas et al., 1995)
EVI	G * ((NIR − R)/(NIR + C1 * R − C2 * B + L))	Enhanced Vegetation Index	(Huete et al., 1997)
REcl	((NIR)/(RE)) − 1	Red-edge Chlorophyll Index	(Gitelson et al., 2005)
MTCI	(NIR − RE)/(RE − R)	MERIS Terrestrial Chlorophyll Index	(Dash and Curran, 2007)
REI	NIR/RE	Red-edge Index	(Gitelson and Merzlyak, 1994)
NDRE3	(RE3 − RE)/(RE3 + RE)	Normalized Difference Red-edge 3	(Barnes et al., 2000)

2.5. Random Forest classification

We chose a Random Forest (RF) classifier as it is known to be superior and reliable for achieving high classification accuracies when compared to other classifiers such as the binary hierarchical classifier, artificial neural networks and decision trees (Belgiu and Drăgu, 2016). Fundamentally, it is an ensemble learning method that is efficient, simple to parametrize, robust, and often used for crop type and cropping pattern mapping (Feyisa et al., 2020; Liu and Chen, 2019; Richard et al., 2017). Based on the spectral analysis and VIs, five random classification scenarios were done viz. (i) all Sentinel-2 spectral bands, (ii) significant spectral bands, (iii) VIs, (iv) all spectral bands and VIs, and (v) significant spectral bands and VIs. We followed Immitzer et al. (2016)'s methodological framework and model parametrization. The sample number of maize and imaize were 50 and 37, respectively. We split the dataset into training and validation sets, 65 % for training and 35 % for validation. The RF has two tuning parameters, the number of trees used to form ensemble denoted by *ntree* and also the number of predictors used for splitting nodes which is denoted as *mtry*. The *mtry* is set to default and it is the square root of the total number of features (Genuer et al., 2010), this parameter plays a significant role in the accuracy of the classification (Breiman, 2001; Saini and Ghosh, 2018). Following a geographically similar study by Richard et al. (2017), we searched for the *ntree* between 500 and 2500 using a 500 interval and optimal maximum depth (max_depth) between 2 and 10 using an interval of 2. The optimal classification results used *ntree* = 50 and max_depth = 4. The random state was set at 5, min_sample_split at 10, and criterion = gini. The RF classifier was implemented using the scikit-learn Library version is 1.2.1 in Python version 3.10.9 (Pedregosa et al., 2011).

3. Results

3.1. Spectral response of maize and imaize during the crop growing season

Fig. 5(a–e) illustrates the spectral response of the two maize cropping patterns during the early crop growing phase until post-harvest period. The spectral reflectance of maize is consistently higher than imaize in bands RE_{705}, RE_{740}, RE_{865} and NIR_{842} for both cropping patterns in vegetative, flowering-yield formation and ripening phases. However, in the same growth phases, maize spectral reflectance is lower than that of imaize in the following bands, 560, 665 and 704 during the emergence-seedling and post-harvest phases, maize spectral reflectance is lower than that of imaize.

The Mann-Whitney test results for the Sentinel-2 spectral bands revealed significant differences in the spectral reflectance of maize and imaize during the vegetative and flowering-yield formation phases across most bands. Particularly, bands like Blue, Green, Red, RE1, RE3, NIR1, and NIR2 exhibit extremely low p-values for both stages, indicating a strong statistical difference in their readings between these two growth stages. As observed in Figs. 5 and 6, differences in spectral reflectance are evident only at the vegetative and flowering-yield formation phases. Specifically, during the vegetative phase, all spectral regions are significantly different ($p < 0.05$), while during the flowering-yield formation, most of the spectral regions show significant differences except for RE_{740}, $SWIR_{1614}$ and $SWIR_{2202}$. The p-values for RE_{740} and $SWIR_{2202}$ during flowering-yield formation are somewhat higher, suggesting a less pronounced but still notable difference. The $SWIR_{1614}$ band has a high p-value in the flowering-yield formation stage, indicating no significant statistical difference in this band between the two stages.

Statistical tests conducted for the emergence-seedling and ripening-harvest growth phases showed no significant differences between the two cropping patterns. This finding is supported by the spectral response

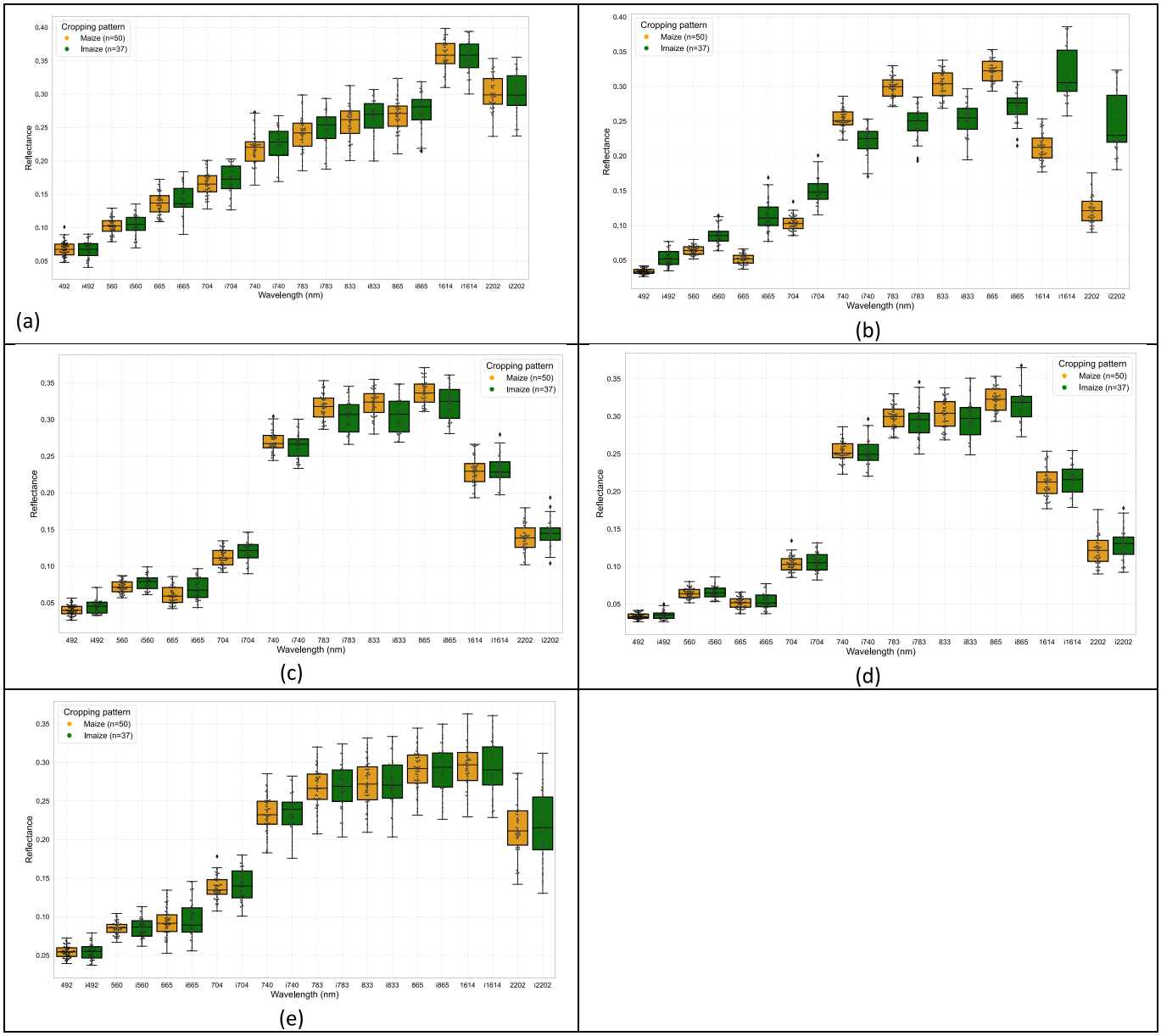

Fig. 5. Boxplots showing the reflectance variation of maize (red) and imaize (blue) in these growth phases (a) emergence-seedling, (b) vegetative, (c) flowering-yield formation, (d) ripening and (e) post-harvest period. (For interpretation of the references to colour in this figure legend, the reader is referred to the web version of this article.)

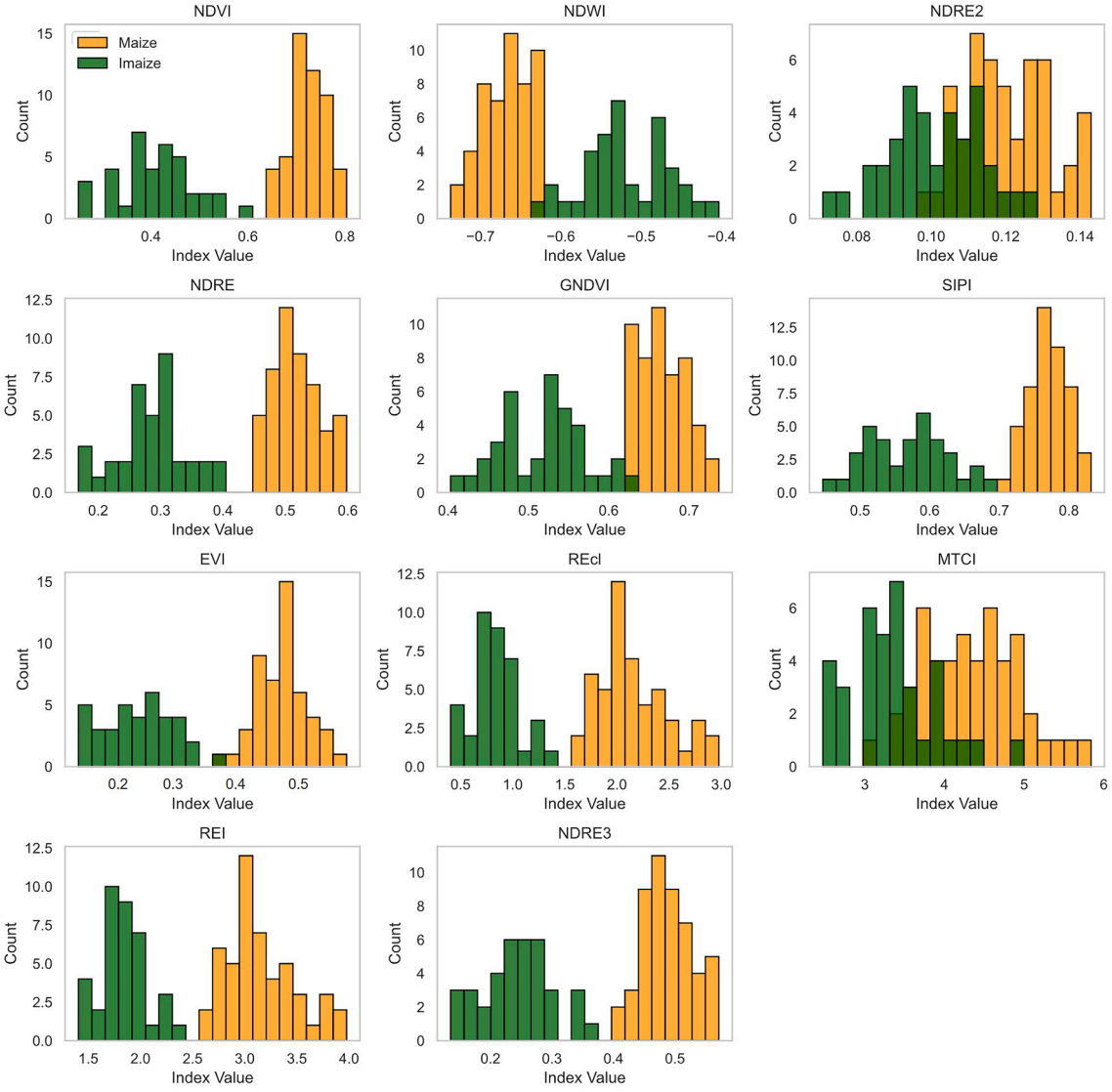

Fig. 6. Histogram plots of the pixel count for each VIs used for discriminating maize and imaize cropping patterns at the vegetative phase.

shown in Fig. 5 (d), where maize and imaize spectral reflectance appears similar across all bands in these phases. The differences during the end of the season were not considered. According to our field interviews, during that period the fields were either fallow, featured cover crops, had a second crop growing (particularly cassava) or early planting for the second season had commenced. These cropping practices are common, leading to the initial stages of a vegetation spectral signature (high NIR and low red reflectance) during this period (Fig. 5 (e)). This analysis suggests that most Sentinel-2 spectral bands are sensitive to changes between the vegetative and flowering-yield stages, with some variations in the degree of sensitivity.

3.2. Analysis of the most suitable VIs for cropping pattern discrimination

The spectral regions that have the potential to discriminate between the two cropping patterns include most spectral regions except RE_{740}, $SWIR_{1610}$, and $SWIR_{2190}$ in flowering-yield formation. The VI analysis in Fig. 6 and Fig. 7 show the frequency distribution of eleven VIs for maize and imaize.

During the vegetative phase, the frequency distributions of the cropping patterns exhibit skewness in different directions with the modes further apart from each other (Fig. 6). For the imaize class, most VIs display a right-skewed distribution, while the maize class shows a left-skewed pattern, except for NDWI. Vegetation indices such as NDRE2, GNDVI, SIPI, NDWI, MTCI and NDVI have few overlaps, whilst EVI, NDRE3, RECL and REI show no overlaps. Overall, there is minimal overlap in the counts between both cropping patterns.

Most of the vegetation indices information for both maize and imaize overlap during the flowering-yield formation phase (Fig. 7). In this phase, most VIs have closely positioned modes, with the exception of NDWI and NDRE2. The distribution of most VIs for maize is skewed to the left, whilst VIs for imaize is slightly skewed to the right. Some VIs, such as NDRE3, GNDVI, NDVI show nearly normal distributions. For maize cropping patterns, RECL, MTCI and NDVI show minor bimodal distributions.

3.3. Random forest classification results

During the vegetative phase, the classification results showed an overall user accuracy, producer accuracy and overall accuracy is 100 % with F1-score and Kc of 1.0 for all the classification scenarios. This is consistent with the spectral analysis and VIs results. The *U* test results reveal significant differences between maize and imaize in this phase. Furthermore, the VIs demonstrated their potential to effectively discriminate between the two cropping patterns during this phase.

For flowering-yield formation phase, the performance of the

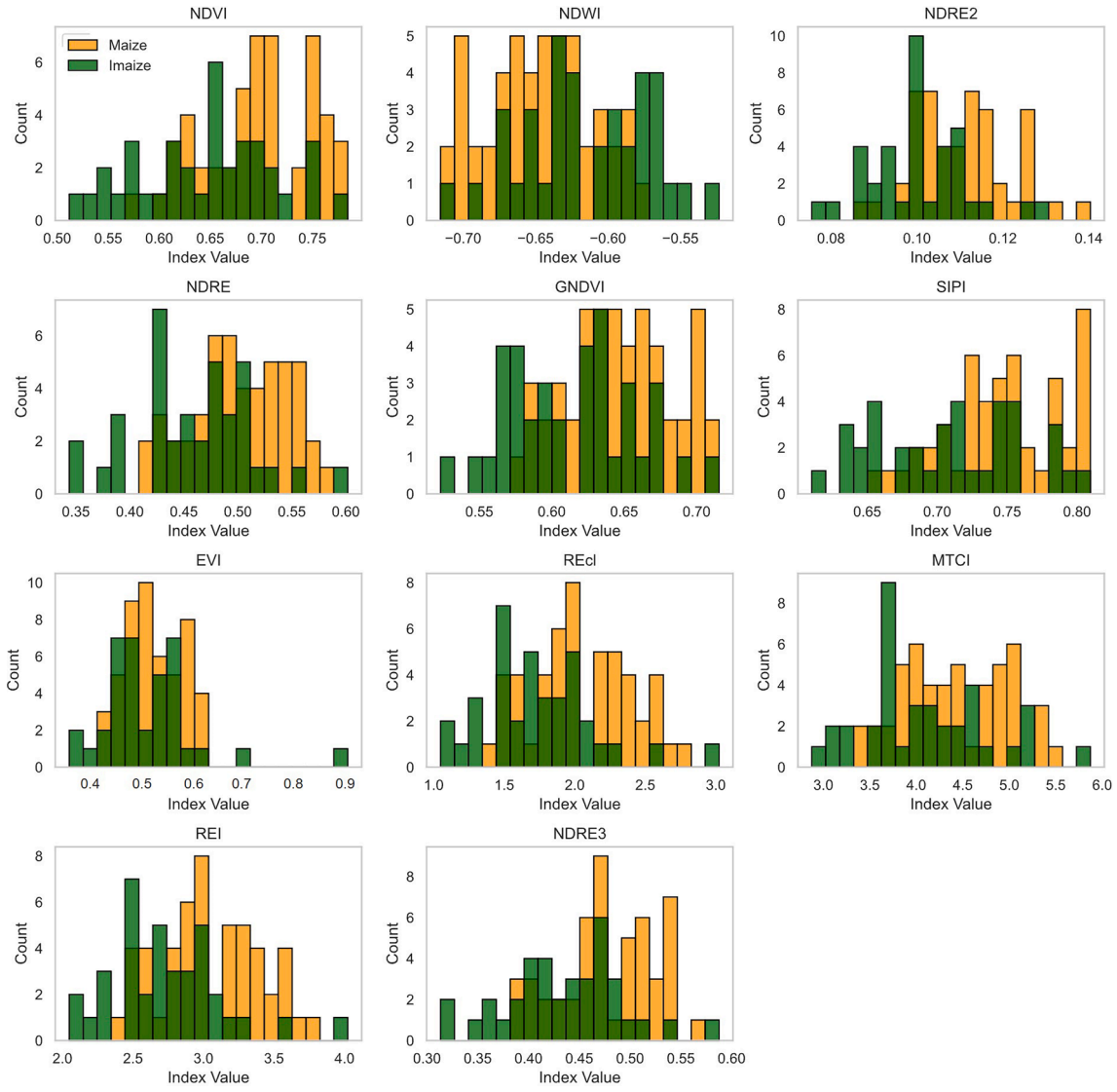

Fig. 7. Histogram plots of the pixel count VIs used for discriminating maize and imaize cropping patterns at flowering-yield formation phases.

combination of (iv) all spectral bands and VI and (v) significant bands and VIs did not surpass that of the other classification scenarios. The highest accuracy was observed in the first three scenarios: (i) all Sentinel-2 spectral bands, (ii) significant spectral bands, (iii) VIs. Specifically, during flowering-yield formation phase, using all spectral bands yielded the highest accuracy of 86 %, followed by significant bands with 79 % and VIs at an overall score of 66 % (Table 4).

4. Discussion

The study demonstrated the utility of temporal Sentinel-2 imagery for the discrimination and classification of maize and intercropped maize fields in rainfed small-holdings of Kenya. The investigation identified key spectral bands, VIs, and growth phases important for accurate discrimination. Spectral data and VIs extracted from five Sentinel-2 images, aligned to the crop calendar were utilized to identify variations between maize and imaize during different growing phases. Our spectral analysis revealed a distinct separation of maize and imaize cropping patterns during the vegetative phase (across all bands) and the flowering-yield phases (specifically in Blue, Green, Red, RE704, RE783, NIR833, NIR865 bands). This distinction proved beneficial for accurate RF classification using Sentinel-2 data from those phases in the region. Regarding VIs, all indices were suitable during the vegetative phase, while in the flowering-yield formation phase, RECL, MTCI and NDVI displyed notable differences alongside some similarities. Despite the study's limitations due to its focus on a relatively small number of test

Table 4
Random forest classification results of flowering-yield formation phase.

Features	Cropping Patterns	User Accuracy	Producer Accuracy	Overall Score	Kappa coefficient	F1-score
All spectral bands	Maize	1.00	0.80	0.86	0.71	0.89
	Imaize	0.69	1.00			0.82
Significant spectral bands	Maize	0.94	0.75	0.79	0.57	0.83
	Imaize	0.62	0.89			0.73
VIs	Maize	0.75	0.67	0.66	0.29	0.71
	Imaize	0.54	0.64			0.58

fields, the results illustrated the potential for discriminating between the two cropping patterns. Additionally, the study highlighted the essential role of utilizing temporal Sentinel-2 spectral data in identifying the critical crop growth phase for mapping cropping patterns with intercropping.

4.1. Differences between maize and imaize spectral response

The overall distribution and median of field-averaged spectral reflectance for maize and imaize were comparatively similar at the emergence-seedling phase (Fig. 5(a)). During this phase, the spectral signature predominantly indicates a mix of soil and crops for both cropping patterns. These results support the earlier findings of Gao et al. (2021), who showed the difficulty in distinguishing crops from the soil, particularly during the early phases of crop growth, such as crop emergence.

During the vegetative phase, the spectral signature of maize and imaize fields is influenced by the planting spacing and the type of intercropping. Significant differences were observed in the distribution and median of reflectance across all spectral regions for both maize cropping patterns. In the red-edge to the near-infrared region, maize has higher spectral reflectance than imaize (Fig. 5 (b)). This difference is due to maize fields having smaller and more uniformly spaced crops. Conversely, in imaize fields, the spacing between plants is wider and less uniform. The variation in spacing is more pronounce in imaize fields, depending on the type of intercropping. For example, the “same hole” planting of maize and beans results in wider spacing, while mixed and row intercropping leads to comparatively smaller spacing between crops (Fig. 2). Furthermore, weeds proliferate in maize fields due to decreased field activity throughout the crop growing season. Conversely, our interviews indicate that farmers are more actively involved in imaize fields than in maize fields, primarily due to the mid-season bean harvest. As a result, weed infestation is less in intercropped maize fields compared to maize fields.

The reflectance distribution and median during the flowering-yield formation phase vary between cropping patterns. Specifically, imaize shows a slightly wider range for most spectral bands compared to maize. Conversely, maize demonstrates higher reflectance in the red-edge and near-infrared regions (Fig. 5 (c)). The high reflectance in maize can be attributed to the presence of weeds within maize fields. This observation aligns with previous study by Lin et al. (2017), which showed similarities in the spectral profiles of maize and weeds,demonstrating that the spectral reflectance values of weeds were higher, especially at the red-edge and near-infrared regions.

During the ripening phase, the reflectance distribution for both cropping patterns showed minimal variation. Across most fields during this phase, mazie was the predominant crop, as intercrops such as beans, soybean and cowpeas had been harvested, with cassava remaining in a few fields. Consequently, the spectral response of maize and imaize became notably similar. This finding aligns with the results reported by Hegarty-Craver et al. (2020), which showed the inability to accurately discriminate between maize and imaize during the later phases of crop growth.

The reflectance values in the post-harvest period remain high for both cropping patterns (Fig. 5(e)). This period is characterized by various agricultural activities, including the cultivation of cassava following bean harvest, ploughing, and the presence of residual maize plants in some maize fields. Additionally, certain maize fields may be covered with weeds, while in certain cases, farmers may have commenced the planting of seeds for the upcoming second crop growing season.

The results of the *U* test revealed that the emergence-seedling, ripening, and post-harvest phases for both maize and imaize showed no significant differences in all spectral regions. These crop growth phases, in both cropping patterns, show no distinct spectral behaviours. Consistent with prior research (Gumma et al., 2020; Hegarty-Craver et al., 2020; Li et al., 2022; Luciani et al., 2019), earlier studies have shown misclassification of cropping patterns due to spectral mixing.

During the vegetative phase, all spectral bands were significantly different between maize and imaize, whilst, during the flowering-yield formation phase, the majority of the spectral regions showed significant differences except for RE_{740}, $SWIR_{1614}$ and $SWIR_{2202}$. Despite these observed significant differences, standard deviations for both cropping patterns during the flowering-yield formation phase showed overlaps indicating shared spectral information in certain fields. This aligns with results by Richard et al. (2017), who, through the use of RapidEye imagery, noted similar spectral responses between maize and imaize cropping patterns during the flowering phase.

4.2. VI analysis

We analysed the variability of commonly used VIs for crop type mapping to assess their effectiveness in discriminating cropping patterns during vegetative and flowering-yield phases. The results during the vegetative phase showed a distinct separation between maize and imaize across all studied VIs (Fig. 6), consistent with spectral reflectance analysis. Similarly, during the flowering-yield phase, some overlaps were observed in VI values for maize and imaize.

The majority of the studied VIs contained either red-edge only or both red-edge and near-infrared bands. Red-edge VIs are valuable in improving crop type classification due to their sensitivity to changes in biophysical and biochemical crop characteristics (Frampton et al., 2013). In comparison to individual spectral bands, VIs are recognized for their capacity to enhance the biophysical and biochemical properties of crops. These characteristics are closely related to properties such chlorophyll, biomass, leaf area index (LAI) and nitrogen content properties (Kang et al., 2021; Kanke et al., 2016). Therefore, these indices prove beneficial for understanding cropping patterns, but their benefits are more pronounced when applied during optimal growth phases for discriminating cropping patterns.

4.3. Classification of maize and imaize at vegetative and flowering-yield formation

The cropping patterns were classified for the vegetative and flowering-yield formation phases. Achieving a 100 % classification accuracy in the seedling-vegetative phase for the studied classification scenarios. The cropping patterns during that period are significantly different, as illustrated by their spectral response (Table 3). The classification model using all spectral bands resulted in higher classification accuracy compared to when using significant spectral bands and VIs as features. Although bands RE_{740}, $SWIR_{1614}$ and $SWIR_{2202}$ were not statistically significant for discriminating the two maize and imaze classes, they still hold subtle information that causes improvement of the classification accuracy when included in the model. These results show the strength of the original Sentinel-2 spectral bands in discriminating crops (Mudereri et al., 2019). The RF classification showed a relatively high accuracy of 87 %, surpassing findings from earlier studies which also utilized RF for crop classification (Chen et al., 2021; Hegarty-Craver et al., 2020; Jin et al., 2019). Several factors, beyond crop growth phase, influenced the results. In comparison to maize ($n = 50$), imaize ($n = 37$) showed lower classification accuracy. This difference may arise from the imbalance sample sizes from the two cropping patterns. While RF is recognized for its superior performance especially when using limited training samples (Belgiu and Drăgu, 2016), it is crucial to note that the model is sensitive to class imbalance.

The increase of training samples, as demonstrated in Ibrahim et al. (2021) study, resulted in improved classification accuracy. Maize classification results achieved the lowest user accuracy (65 %) in their study. However, in this study classification results for maize consistently outperformed those for imaize in all classification scenarios related to user accuracy. These differences in accuracy can be attributed to the

misclassification of maize as imaize, potentially caused by the presence of weeds in maize fields, wherein weeds act as a secondary crop. This challenge is also evident in other studies that classified maize and imaize cropping patterns encountered misclassification due to weeds and high-density legumes in intercropped maize fields (Hegarty-Craver et al., 2020; Ibrahim et al., 2021). Notably, farmers recognized weed infestation as a prevalent challenge, particularly in maize fields. In addressing this issue, manual labour emerged as the primary method for weed removal, given the financial constraints preventing many farmers from affording herbicides. Throughout our field visits, we observed that imaize fields had less weed infestation. As previously highlighted, weed infestation in maize fields is attributed to diminished field activity throughout the crop growing season. Due to the weed infestation problem in such regions, quantitative measurement such as LAI, Soil Plant Analysis Development (SPAD) and fields spectrometer readings can contribute greatly to the understanding of the spectral response of such cropping patterns. The collection of such field data is key for better understanding the spectral response of maize cropping patterns and aid to map intercropping patterns with great detail.

The classification results reported from similar studies displayed inconsistentencies (Feyisa et al., 2020; Hegarty-Craver et al., 2020; Ibrahim et al., 2021; Richard et al., 2017). These inconsistencies may stem from variations in the quantity of field samples, type of imagery utilized, and date of image acquisition. Additional research shared the challenges associated with small and irregularly shaped field sizes in similar settings, thereby adding complexity to the process of mapping crop types and cropping patterns (Burke and Lobell, 2017; Lowder et al., 2016).

The lack of sufficient and relevant field data and optical satellite data that is cloud-free significantly contributes to the challenges of characterising and mapping intercropping. Increasing the number of satellite images through multi-sensor combinations from Landsat, PlanetScope or RapidEye can increase the quantity, spatial and spectral quality to identify subtle reflectance differences that can improve discrimination and classification. Future work could use hyperspectral sensors as they are better suited for distinguishing crops and weeds (Lin et al., 2017).

5. Conclusion

The study's findings illustrates the effectiveness of Sentinel-2 in distinguishing maize and imaize cropping patterns, especially during the vegetative and flowering-yield formation phases. This highlights the necessity of a multi-temporal approach in differentiating cropping patterns that involve intercropping patterns. Through detailed analysis of spectral variations across different crop growth phases, an understanding of the key factors essential for effective discrimination and mapping of cropping patterns has been achieved. These factors include the integration of crop calendar information, thorough temporal analysis, and the utilization of relevant spectral and spatial data. In particular, the red-edge and near-infrared spectral bands have demonstrated their effectiveness in differentiating between cropping patterns that include intercropping. Moreover, the study draws attention to the challenge of weed infestation in maize fields. It highlights how the presence of weeds within maize crops present a unique problem, distinct from the issues posed by intercropping. These weeds behave differently from the intercrop plants, making their detection and management a critical aspect of crop monitoring. Further research and development in this area could lead to more advanced algorithms and models that can accurately identify and discriminate between crops and weeds. Such advancements could significantly enhance the efficiency of cropping pattern management practices, leading to improved yield, reduced labor and resource inputs, and sustainable agricultural practices. Overall, this study contributes valuable insights into the complexities of crop pattern discrimination and the potential of remote sensing technologies in addressing these challenges.

CRediT authorship contribution statement

Mahlayeye Mbali: Writing – review & editing, Writing – original draft, Validation, Methodology, Investigation, Funding acquisition, Formal analysis, Data curation, Conceptualization. **Roshanak Darvishzadeh:** Writing – review & editing, Validation, Supervision, Methodology, Funding acquisition, Conceptualization. **Andrew Nelson:** Writing – review & editing, Supervision, Resources, Methodology, Funding acquisition, Conceptualization.

Declaration of competing interest

The authors declare that they have no known competing financial interests or personal relationships that could have appeared to influence the work reported in this paper.

Data availability

Data will be made available on request.

Acknowledgements

The authors thank the National Research Foundation (NRF) of South Africa and Nuffic for funding the research (grant number: 120226)

References

Aduvukha, G.R., Abdel-Rahman, E.M., Sichangi, A.W., Makokha, G.O., Landmann, T., Mudereri, B.T., Tonnang, H.E.Z., Dubois, T., 2021. Cropping pattern mapping in an agro-natural heterogeneous landscape using Sentinel-2 and Sentinel-1 satellite datasets. Agric. 11, 530. https://doi.org/10.3390/agriculture11060530.

Barnes, E.M., Clarke, T.R., Richards, S.E., Colaizzi, P.D., Haberland, J., Kostrzewski, M., Waller, P., Choi C., R.E., Thompson, T., Lascano, R.J., Li, H., Moran, M.S., 2000. Coincident detection of crop water stress, nitrogen status and canopy density using ground based multispectral data. In: Proc. 5th Int. Conf. Precis Agric.

Bégué, A., Arvor, D., Bellon, B., Betbeder, J., de Abelleyra, D., Ferraz, R.P.D., Lebourgeois, V., Lelong, C., Simões, M., Verón, S.R., 2018. Remote sensing and cropping practices: a review. Remote Sens. 10, 1–32. https://doi.org/10.3390/rs10010099.

Bégué, A., Leroux, L., Soumaré, M., Faure, J.F., Diouf, A.A., Augusseau, X., Touré, L., Tonneau, J.P., 2020. Remote sensing roducts and services in support of agricultural public policies in Africa: overview and challenges. Front. Sustain. Food Syst. 4 https://doi.org/10.3389/fsufs.2020.00058.

Belgiu, M., Bijker, W., Csillik, O., Stein, A., 2021. Phenology-based sample generation for supervised crop type classification. Int. J. Appl. Earth Obs. Geoinf. 95, 102264 https://doi.org/10.1016/j.jag.2020.102264.

Belgiu, M., Csillik, O., 2018. Sentinel-2 cropland mapping using pixel-based and object-based time-weighted dynamic time warping analysis. Remote Sens. Environ. 204, 509–523. https://doi.org/10.1016/j.rse.2017.10.005.

Belgiu, M., Drăgu, L., 2016. Random forest in remote sensing: a review of applications and future directions. ISPRS J. Photogramm. Remote Sens. 114, 24–31. https://doi.org/10.1016/j.isprsjprs.2016.01.011.

Breiman, L.E.O., 2001. Random forests. Mach. Learn. 45, 5–32. https://doi.org/10.1023/A:1010933404324.

Burke, M., Lobell, D.B., 2017. Satellite-based assessment of yield variation and its determinants in smallholder African systems. PNAS 114, 2189–2194. https://doi.org/10.1073/PNAS.1616919114.

Bybee-Finley, K.A., Ryan, M.R., 2018. Advancing intercropping research and practices in industrialized agricultural landscapes. Agric. https://doi.org/10.3390/agriculture8060080.

Castillejo-González, I.L., López-Granados, F., García-Ferrer, A., Manuel, J., Pẽpeña-Barragán, P., Jurado-Expósito, M., Sánchez De La Orden, M., González-Audicana, M., 2009. Computers and Electronics in Agriculture Object-and pixel-based analysis for mapping crops and their agro-environmental associated measures using QuickBird imagery. Comput. Electron. Agric. 68, 207–215. https://doi.org/10.1016/j.compag.2009.06.004.

Chen, C.-R., Chen, C.-F., Son, N.-T., 2014. Rice crop monitoring with multitemporal MODIS-Landsat data fusion. Geophys. Res. Abstr. 16.

Chen, Y., Hou, J., Huang, C., Zhang, Y., Li, X., 2021. Mapping maize area in heterogeneous agricultural landscape with multi-temporal Sentinel-1 and Sentinel-2 images based on random forest. Remote Sens. 13, 2988 https://doi.org/10.3390/RS13152988.

Cui, J., Zhang, X., Wang, W., Wang, L., 2020. Integration of optical and sar remote sensing images for crop-type mapping based on a novel object-oriented feature selection method. Int. J. Agric. Biol. Eng. 13, 178–190. https://doi.org/10.25165/j.ijabe.20201301.5285.

Dash, J., Curran, P.J., 2007. Evaluation of the MERIS terrestrial chlorophyll index (MTCI). Adv. Sp. Res. 39, 100–104. https://doi.org/10.1016/J.ASR.2006.02.034.

Ding, M., Guan, Q., Li, L., Zhang, H., Liu, C., Zhang, L., 2020. Phenology-based rice paddy mapping using multi-source satellite imagery and a fusion algorithm applied to the Poyang Lake plain, Southern China. Remote Sens. 12, 1022 https://doi.org/10.3390/rs12061022.

FAO, 2022. Tobacco | Land & Water | Food and Agriculture Organization of the United Nations | Land & Water | Food and Agriculture Organization of the United Nations [WWW Document]. URL https://www.fao.org/land-water/databases-and-software/crop-information/maize/en/ (accessed 10.10.22).

Ferrant, S., Selles, A., Le Page, M., AlBitar, A., Mermoz, S., Gascoin, S., Bouvet, A., Ahmed, S., Kerr, Y., 2019. Sentinel-1&2 for near real time cropping pattern monitoring in drought prone areas. Application to irrigation water needs in Telangana, South-India. In: International Archives of the Photogrammetry, Remote Sensing and Spatial Information Sciences - ISPRS Archives. International Society for Photogrammetry and Remote Sensing, pp. 285–292. doi: 10.5194/isprs-archives-XLII-3-W6-285-2019.

Feyisa, G.L., Palao, L.K., Nelson, A., Gumma, M.K., Paliwal, A., Win, K.T., Nge, K.H., Johnson, D.E., 2020. Characterizing and mapping cropping patterns in a complex agro-ecosystem: an iterative participatory mapping procedure using machine learning algorithms and MODIS vegetation indices. Comput. Electron. Agric. 175, 105595 https://doi.org/10.1016/j.compag.2020.105595.

Frampton, W.J., Dash, J., Watmough, G., Milton, E.J., 2013. Evaluating the capabilities of Sentinel-2 for quantitative estimation of biophysical variables in vegetation. ISPRS J. Photogramm. Remote Sens. 82, 83–92. https://doi.org/10.1016/j.isprsjprs.2013.04.007.

Gao, F., Anderson, M.C., Johnson, D.M., Seffrin, R., Wardlow, B., Suyker, A., Diao, C., Browning, D.M., 2021. Towards routine mapping of crop emergence within the season using the harmonized landsat and sentinel-2 dataset. Remote Sens. 13 https://doi.org/10.3390/rs13245074.

Garrett, R.D., Ryschawy, J., Bell, L.W., Cortner, O., Ferreira, J., Garik, A.V.N., Gil, J.D.B., Klerkx, L., Moraine, M., Peterson, C.A., Dos Reis, J.C., Valentim, J.F., 2020. Drivers of decoupling and recoupling of crop and livestock systems at farm and territorial scales. Ecol. Soc. 25 https://doi.org/10.5751/ES-11412-250124.

Genuer, R., Poggi, J.M., Tuleau-Malot, C., 2010. Variable selection using random forests. Pattern Recogn. Lett. 31, 2225–2236. https://doi.org/10.1016/j.patrec.2010.03.014.

Giller, K.E., Delaune, T., Silva, J.V., Descheemaeker, K., van de Ven, G., Schut, A.G.T., van Wijk, M., Hammond, J., Hochman, Z., Taulya, G., Chikowo, R., Narayanan, S., Kishore, A., Bresciani, F., Teixeira, H.M., Andersson, J.A., van Ittersum, M.K., 2021a. The future of farming: who will produce our food? Food Secur. 13, 1073–1099. https://doi.org/10.1007/s12571-021-01184-6.

Giller, K.E., Delaune, T., Silva, J.V., van Wijk, M., Hammond, J., Descheemaeker, K., van de Ven, G., Schut, A.G.T., Taulya, G., Chikowo, R., Andersson, J.A., 2021b. Small farms and development in sub-Saharan Africa: farming for food, for income or for lack of better options? Food Secur. 13, 1431–1454. https://doi.org/10.1007/s12571-021-01209-0.

Gitelson, A., Merzlyak, M.N., 1994. Spectral reflectance changes associated with autumn senescence of *Aesculus hippocastanum* L. and *Acer platanoides* L. leaves. Spectral features and relation to chlorophyll estimation. J. Plant Physiol. 143, 286–292. https://doi.org/10.1016/S0176-1617(11)81633-0.

Gitelson, A.A., Merzlyak, M.N., 1998. Remote sensing of chlorophyll concentration in higher plant leaves. Adv. Sp. Res. 22, 689–692. https://doi.org/10.1016/S0273-1177(97)01133-2.

Gitelson, A.A., Viña, A., Ciganda, V., Rundquist, D.C., Arkebauer, T.J., 2005. Remote estimation of canopy chlorophyll content in crops. Geophys. Res. Lett. 32, 1–4. https://doi.org/10.1029/2005GL022688.

Gumma, M.K., Tummala, K., Dixit, S., Collivignarelli, F., Holecz, F., Kolli, R.N., Whitbread, A.M., 2020. Crop type identification and spatial mapping using Sentinel-2 satellite data with focus on field-level information. Geocarto Int. https://doi.org/10.1080/10106049.2020.1805029.

Hegarty-Craver, M., Polly, J., O'Neil, M., Ujeneza, N., Rineer, J., Beach, R.H., Lapidus, D., Temple, D.S., 2020. Remote crop mapping at scale: using satellite imagery and UAV-acquired data as ground truth. Remote Sens. 12, 1–15. https://doi.org/10.3390/rs12121984.

Himmelstein, J., Ares, A., Gallagher, D., Myers, J., 2017. A meta-analysis of intercropping in Africa: impacts on crop yield, farmer income, and integrated pest management effects. Int. J. Agric. Sustain. 15, 1–10. https://doi.org/10.1080/14735903.2016.1242332.

Huete, A.R., Liu, H.Q., Batchily, K., Van Leeuwen, W., 1997. A comparison of vegetation indices over a global set of TM images for EOS-MODIS. Remote Sens. Environ. 59, 440–451. https://doi.org/10.1016/S0034-4257(96)00112-5.

Ibrahim, E.S., Rufin, P., Nill, L., Kamali, B., Nendel, C., Hostert, P., 2021. Mapping crop types and cropping systems in Nigeria with Sentinel-2 imagery. Remote Sens. 13, 1–24. https://doi.org/10.3390/rs13173523.

Immitzer, M., Vuolo, F., Atzberger, C., Sarathi Roy, P., Thenkabail, P.S., 2016. First experience with Sentinel-2 data for crop and tree species classifications in central Europe. Remote Sens. 2016 (8), 166 https://doi.org/10.3390/RS8030166.

Jaeztold, R.S.H., 1983. Farm Management Handbook of Kenya, Vol II, National Conditions and Farm Management Information.

Jin, Z., Azzari, G., You, C., Di Tommaso, S., Aston, S., Burke, M., Lobell, D.B., 2019. Smallholder maize area and yield mapping at national scales with Google Earth Engine. Remote Sens. Environ. 228, 115–128. https://doi.org/10.1016/j.rse.2019.04.016.

Kang, Y., Meng, Q., Liu, M., Zou, Y., Wang, X., 2021. Crop classification based on red edge features analysis of gf-6 wfv data. Sensors 21. https://doi.org/10.3390/s21134328.

Kanke, Y., Tubaña, B., Dalen, M., Harrell, D., 2016. Evaluation of red and red-edge reflectance-based vegetation indices for rice biomass and grain yield prediction models in paddy fields. Precis. Agric. 17, 507–530. https://doi.org/10.1007/s11119-016-9433-1.

Kehs, A., McCloskey, P., Chelal, J., Morr, D., Amakove, S., Plimo, B., Mayieka, J., Ntango, G., Nyongesa, K., Pamba, L., Jeptoo, M., Mugo, J., Tsuma, M., Mukami, W., Onyango, W., Hughes, D., 2021. From village to globe: a dynamic real-time map of African fields through PlantVillage. Front. Sustain. Food Syst. 5, 124. https://doi.org/10.3389/fsufs.2021.514785.

Kross, A., McNairn, H., Lapen, D., Sunohara, M., Champagne, C., 2015. Assessment of RapidEye vegetation indices for estimation of leaf area index and biomass in corn and soybean crops. Int. J. Appl. Earth Obs. Geoinf. 34, 235–248. https://doi.org/10.1016/j.jag.2014.08.002.

Kuchler, P.C., Bégué, A., Simões, M., Gaetano, R., Arvor, D., Ferraz, R.P.D., 2020. Assessing the optimal preprocessing steps of MODIS time series to map cropping systems in Mato Grosso, Brazil. Int. J. Appl. Earth Obs. Geoinf. 92, 102150.

Li, C., Chimimba, E.G., Kambombe, O., Brown, L.A., Chibarabada, T.P., Lu, Y., Anghileri, D., Ngongondo, C., Sheffield, J., Dash, J., 2022. Maize yield estimation in intercropped smallholder fields using satellite data in southern Malawi. Remote Sens. 14, 2458 https://doi.org/10.3390/rs14102458.

Lin, F., Zhang, D., Huang, Y., Wang, X., Chen, X., 2017. Detection of corn and weed species by the combination of spectral, shape and textural features. Sustain. 9 https://doi.org/10.3390/su9081335.

Liu, P., Chen, X., 2019. Intercropping classification from GF-1 and GF-2 satellite imagery using a rotation forest based on an SVM. ISPRS Int. J. Geo-Information 8, 1–20. https://doi.org/10.3390/ijgi8020086.

Liu, M., Wang, M., Wang, J., Li, D., 2013. Comparison of random forest, support vector machine and back propagation neural network for electronic tongue data classification: application to the recognition of orange beverage and Chinese vinegar. Sensors Actuators B Chem. 177, 970–980. https://doi.org/10.1016/J.SNB.2012.11.071.

Lowder, S.K., Skoet, J., Raney, T., 2016. The number, size, and distribution of farms, smallholder farms, and family farms worldwide. World Dev. 87, 16–29. https://doi.org/10.1016/j.worlddev.2015.10.041.

Luciani, R., Laneve, G., Jahjah, M., 2019. Agricultural monitoring, an automatic procedure for crop mapping and yield estimation: the great rift valley of Kenya case. IEEE J. Sel. Top. Appl. Earth Obs. Remote Sens. 12, 2196–2208. https://doi.org/10.1109/JSTARS.2019.2921437.

Mahlayeye, M., Darvishzadeh, R., Nelson, A., 2022. Cropping patterns of annual crops: a remote sensing review. Remote Sens. https://doi.org/10.3390/rs14102404.

McFeeters, S.K., 1996. The use of the Normalized Difference Water Index (NDWI) in the delineation of open water features. Int. J. Remote Sens. 17, 1425–1432. https://doi.org/10.1080/01431169608948714.

Mthembu, B.E., Everson, T.M., Everson, C.S., 2019. Intercropping for enhancement and provisioning of ecosystem services in smallholder, rural farming systems in KwaZulu-Natal Province, South Africa: a review. J. Crop Improv. 33, 145–176. https://doi.org/10.1080/15427528.2018.1547806.

Mudereri, B.T., Dube, T., Adel-Rahman, E.M., Niassy, S., Kimathi, E., Khan, Z., Landmann, T., 2019. A comparative analysis of planetscope and sentinel sentinel-2 space-borne sensors in mapping striga weed using guided regularised random forest classification ensemble. Int. Arch. Photogramm. Remote Sens Spat. Inf. Sci. - ISPRS Arch. 42, 701–708. https://doi.org/10.5194/isprs-archives-XLII-2-W13-701-2019.

Pedregosa, F.G., Varoquaux, A., Gramfort, V., Michel, B., Thirion, O., Grisel, M., Blondel, A.E., 2011. Scikit-Learn: machine learning in Python. J. Mach. Learn. Res. 55, 2825–2830.

Peña-Barragán, J.M., Ngugi, M.K., Plant, R.E., Six, J., 2011. Object-based crop identification using multiple vegetation indices, textural features and crop phenology. Remote Sens. Environ. 115, 1301–1316. https://doi.org/10.1016/J.RSE.2011.01.009.

Peñuelas, J., Baret, F., Filella, I., 1995. Semiempirical indexes to assess carotenoids Chlorophyll-a ratio from leaf spectral reflectance. Photosynthetica 31, 221–230.

Plant Village, 2019. PlantVillage Kenya Ground Reference Crop Type Dataset. Version 1.0, Radiant MLHub. [1 October 2022] .https://doi.org/10.34911/rdnt.u41j87.

Plant Village, 2023. URL https://plantvillage.psu.edu/ (accessed 12.7.23).

Richard, K., Abdel-Rahman, E.M., Subramanian, S., Nyasani, J.O., Thiel, M., Jozani, H., Borgemeister, C., Landmann, T., 2017. Maize cropping systems mapping using RapidEye observations in agro-ecological landscapes in Kenya. Sensors (Switzerland) 17, 2537. https://doi.org/10.3390/s17112537.

Rouse, J.W., Hass, R.H., Schell, J.A., Deering, D.W., 1973. Monitoring vegetation systems in the Great Plains with ERTS. In: Nasa ERTS Symposium, pp. 309–313.

Saini, R., Ghosh, S.K., 2018. Crop classification on single date Sentinel-2 imagery using random forest and suppor vector machine. Int. Arch. Photogramm. Remote. Sens. Spat. Inf. Sci. XLII-5, 683–688. https://doi.org/10.5194/isprs-archives-xlii-5-683-2018.

Song, Q., Zhou, Q., Wu, W., Hu, Q., Lu, M., Liu, S., 2017. Mapping regional cropping patterns by using GF-1 WFV sensor data. J. Integr. Agric. 16, 337–347. https://doi.org/10.1016/S2095-3119(16)61392-8.

Sun, R., Chen, S., Su, H., Mi, C., Jin, N., 2019. The effect of NDVI time series density derived from spatiotemporal fusion of multisource remote sensing data on crop classification accuracy. ISPRS Int. J. Geo-Inf. 8, 502. https://doi.org/10.3390/ijgi8110502.

Yang, T., Siddique, K.H.M., Liu, K., 2020. Cropping systems in agriculture and their impact on soil health-a review. Glob. Ecol. Conserv. 23, e01118 https://doi.org/10.1016/j.gecco.2020.e01118.

Zaefarian, F., Rezvani, M., 2016. Soybean (*Glycine max* [L.] Merr.) production under organic and traditional farming. In: Environmental Stresses in Soybean Production: Soybean Production. Academic Press, pp. 103–129. doi: 10.1016/B978-0-12-801535-3.00005-X.

Zuo, L.J., Wang, X., Liu, F., Yi, L., 2013. Spatial exploration of multiple cropping efficiency in china based on time series remote sensing data and econometric model. J. Integr. Agric. 12, 903–913. https://doi.org/10.1016/S2095-3119(13)60308-1.